

Reply to Reviewers' Comments (bg-2017-509) by Weng et al.

Dear Associate Editor and Reviewers:

We have carefully prepared our response and revised our manuscript accordingly. Some major revisions made in the main text can be found in: P2 L1-15; P13 L6-22; P14 L1-5; P15 L1-18; P16 L5-14; P17 L3-5 (rephrased). Some minor revisions made in the main text are in: P6 L9; P8 L20-21; P9 L8-9; P9 L16; P12 L6; P14 L6-22; P15 L22; P16 L16. Please check the revised manuscript for details in the attachment. Two figures are added into the supplementary information.

Our rebuttal letter is lengthy, and we appreciate the patience of Associate Editor, Reviewer#1 and Reviewer#2. Abbreviation used here are: organic carbon (OC), short-range-order (SRO), soil organic matter (SOM), soil organic carbon (SOC)

Response to Reviewer#1:

We use an old (3500 years) pyrogenic OC-mineral consortium to demo the in-situ OC-mineral interplay in a relatively simple mineralogy context. In-situ evidence reveals abundant mineral nano particles, in dense thin layers or nano-aggregates/clusters, instead of crystalline, micron or clay-size minerals on or near OC surfaces, the key working minerals for C stabilization are essentially SRO minerals and/or poorly crystalline submicron size clay minerals. Supported by FTIR spectroscopic results, the studied OC is not merely in criss-cross co-localization with reactive SRO minerals. There is a significant degree of binding between OC and minerals. We also have other sets of unpublished 3-D tomography data for samples from various mineralogy background, and the minerals found associated with OC surface are coincidentally in line with nano particles/poorly crystalline minerals. 'Mineral physical protection for OC stabilization may be more important than previously thought' is not a solid conclusion, the statement is deleted.

Technology Progress for In-Situ Evidence:

This high resolution 3-D tomography tool we introduce has unprecedented resolution, is promising for new insight on in-situ organo-mineral association, the interior 3-D structure of microaggregates, and the fate of mineral nano particles including heavy metals in natural environment. Though some 3-D tomography research have been done on soil microstructure and porosity using X-ray micro-CT, the best achieved resolution only reaches tens of microns (Quin et al., 2014 (with biochar amendment, 70 microns); Kravchenko et al., 2015 (13 microns)), which exceeds the size of clay minerals (<2 microns), and not fit for capturing the microstructure of clay, and the submicron

assemblage of SRO minerals such as Fe oxyhydroxides.

High resolution X-ray scanning and 3-D tomography is highly demanding in terms of technology, multidisciplinary and big-data analysis (Lafond et al., 2015). Except for the adoption of high resolution X-ray objective, fidelity of 3D tomography relies on the accurate alignment of the 2D projections in correct three-dimensional positions. However, non-negligible mechanical imperfection of the rotational stages at nanometer level, or the thermal effects may significantly degrade the spatial resolution of reconstructed tomography. We've developed a markerless image auto-alignment algorithm for fast projection matching (**Faproma**, Wang et al., 2017) to surpass these difficulties, and accomplished accurate reconstruction of 3-D tomography down to nano meters.

Carbon Stabilization:

Soil organic C can be: (1) physically stabilized, or protected from decomposition, through microaggregation; or (2) intimate association with silt and clay particles in organo-mineral complexes; and (3) can be biochemically stabilized through the formation of recalcitrant SOC compounds (Six et al., 2002). Three main mechanisms of Soil organic matter stabilization are: (1) chemical stabilization, result of chemical or physiochemical binding between SOC and soil minerals (especially clay and silt in current opinions), aka organo-mineral complexation; (2) physical protection, which is predominantly at the microaggregate level, built on top of chemical organo-mineral complexation, and (3) biochemical stabilization, which is often experimentally defined, or equated to the nonhydrolyzable fraction (Stevenson, 1994; Christensen, 1996; Six et al., 2002). Experimentally to quantify C of different stabilized levels, a size/density fractionation approach with external force is routinely used for bulk soil, and three or more density fractions are divided: (a) free particulate OM; (b) occluded particulate OM; and (c) colloidal or clay associated OM, in the fine and dense fraction (Golchin et al., 1994, Sollins et al., 2009).

The stabilization of OC by the soil matrix is considered a function of the chemical nature of specific soil mineral fraction, the presence of multivalent cations, the presence of mineral surfaces capable of adsorbing organic materials, and the micro architecture of the soil matrix (Edwards and Bremner, 1967). The degree and amount of protection attributed by each mechanism depends on the chemical and physical properties of mineral matrix, the morphology, chemical nature and structure of organic matter (Baldock and Skjemstad, 2000). However, each mineral's unique capacity to stabilize organic C is rarely recognized in bulk sample analysis, or within size/density fraction. Thus, quantifying the protective capacity of a soil requires a careful consideration of all mechanisms of protection and the implications of experimental procedures.

It is found that accumulation and subsequent loss of organic C were largely driven by changes in the millennial scale cycling of mineral-stabilized carbon (Torn et al., 1997, *Nature*). The protection of SOC by silt and clay particles in soils is well established for a positive relationship between old/stabilized organic C and the content of silt and/or clay in fine and dense fraction (Sorensen, 1972; Feller and Beare, 1997; Hassink, 1997; Trumbore, 1997). In addition to the clay content, clay type (2:1 vs 1:1 clay vs allophanic /short-range-order (SRO) minerals) has strong influence on the stabilization of organic C (Torn et al., 1997). Yet little is known about how spatial and temporal variation in soil mineralogy (especially type, phase, reactivity) controls C long term stabilization in terms of quantity and turnover (Oades, 1994, Torn et al., 1997). Quantification of interactive relationships is imperative, measurement and information using 2-D and 3-D quantitative tool will have great benefit in understanding soil C and aggregate dynamics (Six et al., 2004).

Very limited information is available on the in-situ distribution of clay-size or reactive minerals in soil, and subsequent organo-mineral micro assemblage in soils. For example, a substantial parts of mineral surfaces are considered likely not covered by organic matter (Ransom et al. 1998; Arnarson and Keil 2001; Mayer and Xing 2001; Kahle et al. 2002). Recently, nano scale two-dimensional mapping using Nano SIMS generated direct evidence, revealing that less than 19 percent of the clay-sized mineral surfaces co-localize with OC (Vogel et al., 2014, *Nature Communication*). Views of carbon sequestration in soils and the widely used carbon saturation estimates have been revolutionized to recognize likely only a limited proportion of the clay-sized surfaces contribute to OM sequestration in real soil environment. However, this research could underestimate the actual contact surface area between OC and mineral due to the limitation of sample treatment and two-dimensional approach. Exactly which reactive mineral in the clay-sized fraction interact with OC remains unknown.

The cornerstone research done by Torn et al. (1997) revealed a positive relationship between non-crystalline minerals and organic carbon in soils through the climate gradient. In couple with extraction using ammonium oxalate and/or sodium dithionite-citrate-bicarbonate (DCB), SRO minerals, which may only be a small portion in the fine and dense fraction, are found of great importance for C stabilization, and further discovered preferentially associated with aromatic/lignin-like C (Kaiser et al., 2002; Eusterhues et al., 2005; Kleber et al., 2005; Mikutta et al., 2005, 2006, 2007; Rasmussen et al., 2005; Schneider et al., 2010; Cusack et al., 2012). The SRO minerals are known of high reactivity due to small size, large surface area and charges, their encounter with reactive OC surface may develop strong organo-mineral complexation (Eusterhues et al., 2008, 2011). Yet, the actual key mineral player (micron size clay vs nano scale SRO minerals) for interaction with OC, and their **spatial and temporal variation** is not

known in real soil environment (Vogel et al., 2014). On the other hand, a three-dimensional functional view of carbon turnover dynamics at the microscale has gained ground (Kleber et al., 2018), which consider a multitude of largely independent microreactors within the soil. For example, anaerobic microsites are discovered of great importance for C stabilization (Keiluweit et al., 2017). New perspectives call for observational evidence on OC-mineral micro assemblage in details at nano scale.

Using high resolution 3-D tomography and synchrotron-based spectroscopic approach, we unveil:

- i) There is a high heterogeneity within OC-mineral consortium, including many nano/submicron size mineral particles, porosity and microsites.
- ii) Most of the particulate OC surface is coated by minerals.
- iii) The minerals on the OC-mineral interplay surface are essentially nano size SRO minerals, and or submicron poorly crystalline clay minerals, which are highly reactive and may have large surface for C absorption.
- iv) Very few micron size/clay-size, euhedral/crystalline minerals are observed.
- v) The 3500-year-old pyrogenic OC is highly aromatic (1596 and 1386 cm^{-1}), when at the same time has highly reactive carboxyl functional group (1706 cm^{-1}).
- vi) Broad FTIR bands indicate a significant degree of organo-mineral association between OC and SRO minerals, which are not just criss-cross co-localization.
- vii) The OC surface is often coated by dense and thin layers of mineral nano particles, pointing to likely mineral absorption.
- viii) Within regions microns from particulate OC surface, abundant mineral nano particles develop nano-aggregates/clusters, pointing to likely OC-mineral co-precipitation.

Our results suggest:

- i) The coated particulate OC surfaces by SRO mineral nano particles are stabilized.
- ii) Minerals physical protection contributes to the long term persistence of OC (3500-year-old) in the sub-tropical environment.
- iii) Substantial mineral surfaces are likely available for C stabilization.
- iv) Large amount of nano-aggregates/clusters likely interact/co-precipitate with relatively free OC, which is difficult to prove directly.
- v) Current electron microscopy/spectroscopy/fractionation approach focusing on clay-sized mineral may lead to underestimation of C stabilization attributed by mineral physical protection.

We propose:

- i) High resolution 3-D tomography is a powerful, suitable tool for nailing down the correct key working minerals for C stabilization.
- ii) Two-dimensional TEM may be applicable in revealing nano particles, amorphous/poorly crystalline minerals, on certain focal plane, but not for a whole view.
- iii) XRD is powerful for detecting crystalline minerals but very poor in resolving SRO minerals, cautions should be taken in sample preparation and mineralogy pattern interpretation.
- iv) More research should be done to prove: i) whether it is a general phenomenon that the minerals interact with OC are essentially nano particle SRO minerals and or poorly crystalline submicron size clay minerals, ii) whether the major mineral for C stabilization is nano size SRO minerals instead of clay-sized minerals.
- v) Perspective on SOM dynamics may have to take account the role of SRO minerals into modelling parameters, instead of drawing conclusion mainly on clay type and content (Kleber et al., 2010).

Carbon Models and Carbon Saturation:

Most current models of SOM dynamics try to describe soil heterogeneity by defining several pools, typically three to five, experimentally applicable with supposed different intrinsic decay rates. Meanwhile, first order kinetics are assumed for the decomposition of different conceptual pools (Parton, et al., 1994; Paustian, 1994; McGill, 1996), which infers equilibrium C stocks are linearly proportional to C inputs (Paustian et al., 1997). These models predict that soil C stocks can theoretically be increased without limit, provided that C inputs increase without limit, leading to no assumptions of soil C saturation. Such models have been largely successful in representing SOM dynamics under some studied conditions and management practices, and native soils (e.g. Parton et al., 1987, 1994; Paustian et al., 1992; Powlson et al., 1996). Notably, the representation of the model pools (or quality spectrum) is primarily conceptual in nature (Christensen, 1996; Elliott et al., 1996; Six et al., 2002). The individual pools are generally only loosely associated with measurable quantities obtained with existing analytical methods. The notion of carbon saturation is developed on the assumption that mineral physical protection could be limited by soil physiochemical characteristics such as silt and/or clay content, microaggregate, and surface area (Kemper and Koch, 1966; Hassink, 1997). Six et al. (2002) proposed a conceptual model which use the physicochemical characteristics inherent to soils to define the maximum protective capacity of different SOC pools, which may limit the increases in C sequestration with

increasing organic residue inputs. This conceptual model includes four measurable pools: (1) a biochemically-protected C pool; (2) a silt and clay-protected C pool (less than 53 micron organomineral complexes); (3) a microaggregate-protected C pool (53 to 250 micron aggregates); and (4) an unprotected C pool. Each pool is supposed to have its own dynamics and stabilizing mechanism, which is in turn hypothesized to determine a level at which soil C becomes saturated. The silt and clay protected C pool, which is protected by association with the mineral particles, is defined as hydrolysable fraction and the biochemically-protected C pool is experimentally defined as nonhydrolyzable fraction. Biochemical stabilization is understood as the stabilization of SOM due to its own chemical composition (e.g. recalcitrant compounds such as lignin and polyphenols) and through chemical complexing processes (e.g. condensation reactions) in soil. The unprotected C pool is considered labile, an important nutrient source, which is very sensitive to management practices. Interestingly, the hierarchy for carbon stabilization based on protection capacity/level, from low to high has been ranked as: silt + clay protected pool, microaggregate protected pool, biochemically protected, and non-protected pool on the top to cap the maximum carbon saturation.

Six et al. (2002) pointed that there are major gaps in knowledge and proposed a research priority in terms of soil C saturation on mechanistic level, **if it exists**, especially for unprotected and biochemically protection pools.

As an outsider, we share a few points:

- i) The heterogeneity of microaggregates is little understood and minimal quantitative data is available.
- ii) The unprotected pool actually involves some mechanism separation and dispersion, which is not truly unprotected.
- iii) Six et al. (2002) shared our thought that non-hydrolyzable fraction is not only biochemically stabilized but is also partially stabilized by association with clay and silt particles, and the silt and clay protected pool could also be partially stabilized by incorporation in microaggregates.
- iv) The aged pyrogenic OC (3500-year-old) in our study is not only biochemically stable, but also partially stabilized by association with submicron minerals.

Reviewer #1 suggested some interesting research on biochemically stabilized organic compounds free of minerals, which appears a large expansion to very solid organic geochemistry. Many models for SOM dynamics indeed incorporate a huge 'inert' but relatively uncharacterized pool, which may include biochemically stabilized organic compounds free of minerals, or not. Perspective on carbon stabilization may have to expand from a time scale of centennials and millenniums to an even longer geological

time scale in current C saturation models. Derenne et al. (1991) carried out research on biochemically stabilized organic compounds free of minerals, especially on kerogen/fossil-like organic compounds, in the perspective of kerogen/fossil biochemical transformation, condensation and formation. It takes millions of years for the formation and transformation of kerogen/fossil-like organic compounds. We suggest research on biochemically protected pool also expand into black carbon/pyrogenic organic carbon, which are biochemically stable due to their high aromaticity, have similar chemistry and structure with kerogen and coal, and can persist over millenniums under natural exposure. Long term abiotic/biotic degradation, aerobic/anaerobic alteration can render development of reactive surface functional groups (Liang et al., 2006), and lead to consequent mineral physical protection and C stabilization over millenniums, even in the topical environment (Liang et al., 2008).

Response to Reviewer#2:

We thank Reviewer #2 for recognizing our work in methodology development and contribution to the understanding of C stabilization. In-situ evidence reveals abundant mineral nano particles, in dense thin layers or nano-aggregates/clusters, instead of crystalline micron/clay-size mineral on or near OC surfaces. The key working minerals for C stabilization are essentially nano size SRO minerals and/or poorly crystalline submicron size clay minerals. Inspired by reviewer's suggestions, efforts have been taken to identify micro assemblage features which indicate adsorption or co-precipitation in our natural OC-mineral consortium using TXM images. In the all-depth 2-D X-ray absorption-contrast image (Fig. S2), sheet-like mineral coating is observed on OC surface, which is a dense and thin layer, pointing to likely a high level of physical protection. We propose such texture originate from absorption. Another distinct texture is recognized as OC-mineral nano-aggregates/clusters, with either minerals in the core and OC around (Fig. S2), or vice versa (Fig. S3). This type of texture indicates possible OC-mineral co-precipitation at microsites. Many clusters of various shapes are observed (Fig. S3). However, to fully explore this long-standing question on the structural development of OC-Fe mineral assemblages attributed by absorption vs co-precipitation, we suggest future research with carefully designed samples (such as distinct lab-made OC-Fe consortiums) and enough 3-D tomography observations are needed for reliable evidence and answers.

We've added Figures S2 and S3 into the supplementary information, please check for details, thank you.

1 **Mineral physical protection and carbon stabilization in-situ evidence**
2 **revealed by nano scale 3-D tomography**

3 Yi-Tse Weng^{1,#}, Chun-Chieh Wang^{2,#}, Cheng-Cheng Chiang², Heng Tsai³, Yen-Fang
4 Song², Shih-Tsuen Huang⁴, Biqing Liang^{1,*}

5 ¹National Cheng Kung University, Department of Earth Sciences, Tainan, Taiwan ROC

6 ²National Synchrotron Resource Research Center, Hsinchu, Taiwan ROC

7 ³National Changhua University of Education, Department of Geography, Changhua,
8 Taiwan ROC

9 ⁴National Taichung University of Education, Department of Science Education and
10 Application, Taichung, Taiwan ROC

11 #Equal Contribution

12 *Corresponding author: Biqing Liang
13 (liangglobalcarbon@gmail.com;liangbq@mail.ncku.edu.tw)

14
15 **Abstract**

16 An approach for nano scale 3-D tomography of organic carbon (OC) and
17 associated mineral nano particles was developed to illustrate their spatial distribution and
18 boundary interplay, using synchrotron-based transmission X-ray microscopy (TXM). The
19 proposed 3-D tomography technique was first applied to in-situ observation of a lab-made
20 consortium of black carbon (BC) and nano mineral (TiO₂, 15 nm), and its performance
21 was evaluated under dual-scan absorption contrast and phase contrast modes. Then this
22 novel tool was successfully applied to a natural OC-mineral consortium from high
23 mountain soil at a spatial resolution down to 60 nm, showing the fine structure and
24 boundary of OC, distribution of abundant minerals at nano size, and in-situ 3-D organo-
25 mineral association. The stabilization of aged natural OC was found [mainly](#) attributed to

1 the physical protection of [nano size](#) Fe-containing minerals (Fe oxyhydroxides including
2 ferrihydrite, goethite, and lepidocrocite), and the strong organo-mineral complexation. [In-](#)
3 [situ evidence reveals abundant mineral nano particles, in dense thin layers or nano-](#)
4 [aggregates/clusters, instead of crystalline clay-size minerals on or near OC surfaces. The](#)
5 [key working minerals for C stabilization are essentially reactive short-range-order \(SRO\)](#)
6 [mineral nano particles and/or poorly crystalline submicron size clay minerals. The](#)
7 [sorption of OC to SRO mineral \(or vice versa\) through organo-mineral multiple complex](#)
8 [bonds could occupy and consume their respective reactive surface sites, leading to](#)
9 [enhanced stabilization.](#) The ubiquity~~ousness~~ and abundance of mineral nano particles [on](#)
10 [OC surface](#), and their heterogeneity in natural environment could have been seriously
11 underestimated by traditional study approach. Our in-situ description of organo-mineral
12 interplay at nano scale provides direct evidence to substantiate the importance of mineral
13 physical protection for OC long term stabilization. ~~Mineral physical protection for OC~~
14 ~~stabilization may be more important than previous understanding.~~ This high resolution 3-
15 D tomography tool is promising for new insight on the interior 3-D structure of micro-
16 aggregates, in-situ organo-mineral interplay, and the fate of mineral nano particles
17 including heavy metals in natural environment.

18

19

20 **Introduction**

1 Mineral association with organic carbon (OC) may be an important stabilization
2 mechanism for carbon long-term sequestration, yet little is known about their in-situ
3 interplay and extent of association on aggregation level either chemically or physically
4 (Baldock and Skjemstad, 2000; Cusack et al., 2012; Mikutta et al., 2006; Torn et al., 1997;
5 Vogel et al., 2014). Traditional fractionation methods based on size and external force for
6 dissecting the association strength between OC and minerals in soils are limited to bulk
7 sample. High resolution information and in-situ knowledge is required for interpretation of
8 fractionation results and modeling (Kaiser et al., 2002; Kleber et al., 2007; Sollins et al.,
9 2009). Nano scale two-dimensional isotopic mapping discovered that only a limited
10 amount of the clay-sized surfaces contributed to OC sequestration (Vogel et al., 2014).
11 Understanding OC interplay with minerals in the fine fraction warrants study in a three
12 dimensional way (Kinyangi et al., 2006; Lehmann et al., 2007; Lehmann et al., 2008;
13 Solomon et al., 2012). Detailed in-situ association information between OC and minerals
14 may lead to breakthrough on mineral physical protection mechanism for OC long term
15 stabilization. To overcome the limitations of commonly used electron microscopic
16 methods (such as only on the surface layer, and undesirable artifacts due to
17 pretreatments), non-destructive high-resolution X-ray 3-D tomographic technique will be
18 used for exploring the fine structure of OC and boundary interplay with mineral nano
19 particles.

20 High resolution Synchrotron-based TXM has been demonstrated as a powerful
21 tool for understanding the internal 3-D structure of particles down to nano meter scale,
22 due to its large penetration depth and superior spatial resolution (Kuo et al., 2011; Wang

1 et al., 2015). This technique was successfully applied to reveal the discrete three
2 dimensional micro-aggregation structure of clay (kaolinite) in natural aqueous
3 environment, and generated remarkable tomography that revealed precise inter-particle
4 structure (Zbik et al., 2008). Clay particles with diameter below 500 nm were clearly visible
5 and their pseudo-hexagonal symmetry was recognized in details in a three dimensional
6 way.

7 The synchrotron-based TXM at the beamline BL01B1 of Taiwan Light Source
8 (TLS), which has been used in this study, provides two-dimensional imaging and three-
9 dimensional tomography at a spatial resolution of 30/60-nm with tunable energy (8-
10 11keV). It provides unprecedented opportunity for studying OC boundary interplays with
11 mineral particles at nano meter scale. Two image acquisition modes, absorption contrast
12 and phase contrast, can be used alternatively for recognizing OC and nano minerals.
13 Conventionally, X-ray images are taken in the absorption contrast mode, and the resulting
14 image contrast only depends on the difference of X-ray attenuation coefficient between
15 materials. This mode is especially useful for materials consisted of high atomic number
16 compositions. However, in organic materials, the difference of X-ray attenuation
17 coefficients between specimen and air is too small to distinguish each other. For this
18 reason, the structure of organic materials is often hard to be recognized due to low
19 contrast in absorption contrast images. Alternatively, phase contrast technique transfers
20 optical path length differences (optical phase) inside specimens into intensity contrast,
21 can be used for imaging low atomic number materials, which are poor to absorb X-rays.
22 It provides a unique opportunity to observe fine structures of organic specimens such as

1 OC. Little study has been done on OC and mineral nano particles using high-resolution
2 3-D X-ray tomography, though non-synchrotron-based 3-D X-ray microscopy was used
3 to observe occluded carbon in phytolith structure and kerogen in micrometer scale
4 (Alexandre et al., 2015; Bousige et al., 2016). We aim to develop a new dual-scan method
5 using phase contrast and absorption contrast modes of the TXM alternatively for the
6 observation of OC and mineral consortiums inside lab-made and natural samples in nano
7 meter scale. Lab-made OC in forms of black carbon (BC) will be examined in the artificial
8 consortium with added nano mineral (TiO₂) particles using synchrotron-based TXM for
9 the first time.

10 Black C/biochar has received increasing research interest globally due to its
11 importance in global carbon cycling, soil fertility improvement and environmental pollutant
12 remediation (Bond et al., 2013; Jeffery et al., 2015; Kuhlbusch, 1998; Lehmann et al.,
13 2007; Liang et al., 2006; Liang et al., 2008; Schmidt, 2004). On top of method
14 development for 3-D tomography at nano meter scale, this study provides in-situ
15 evidences on the minerals physical protection on natural OC, and to explore the C
16 stabilization mechanism in natural soil.

17

18 **Methodology**

19 **Sample preparation and background**

20 Black C was made in lab using leguminous plant (*Sesbania roxburghii*) of 80 days'
21 harvest, which was first oven-dried (65 °C) and charred inside a muffle furnace at 300 °C

1 in loosely sealed stainless containers (Chen et al., 2014b). This consortium of low
2 temperature BC and mineral nano particles was constructed by dry deposition of
3 commercial TiO₂ (15 nm) on lab-made BC (3 mm chunk), and then embedded in Gatan
4 G-1 epoxy. The block were cross sectioned to a thickness of 100 to 200 μm using a
5 microtome (Leica Reichert Ultracut E ultra-microtome) and subsequently hand-polished
6 to a thickness of 30 to 50 μm. Each section was transferred onto Kapton tape and
7 mounted on a stainless steel sample holder for TXM observation. Before TXM analysis,
8 gold nano particles (50-150 nm or 400-500 nm in diameter) were deployed on the section
9 surface for image registration ~~before 3-D tomography reconstruction~~.

10 Thin section of natural OC and mineral consortium (NH) was prepared using
11 micron to millimeter size particulate sample from high mountain soil. Particulate organic
12 matter of mm-size with minerals embedded inside was taken from the lower dark layer at
13 depth of 72-93 cm in a Typic Humicryepts soil profile, located in Mt. Nanhua, Nantou
14 County, Taiwan (24°03'00", 121°17'02"). On top of this dark layer, iron stain was observed
15 within the depth of 63-72 cm in the profile. The soil has developed on top of sandstone
16 and slate, with some features of inceptisol and spodosol. The sampling elevation is 3092
17 m, the annual temperature is 7.57 °C, and the yearly rainfall is 2203.1 mm. The major
18 vegetation is arrow bamboo (*Yushania nittakayamensis*), with sporadic Hemlock (*Tsuga*
19 *chinensis*), fir (*Abies kawakamii*), and spruce (*Picea morrisonicola*).

20 The sequestration environment represents weak leaching and inactive chemical
21 weathering conditions. The age of soil organic C has been estimated to 3500 years B.P.

1

2 **Working conditions of TXM**

3 A superconducting wavelength shifter source provides a photon flux of 4×10^{11}
4 photons s^{-1} (0.1% bw) $^{-1}$ in the energy range of 5-20 KeV at the BL01B1 beamline. A
5 double crystal monochromator exploiting a pair of Ge (111) crystals selects X-rays within
6 the energy range of 8-11 KeV. The specimen is imaged using a Fresnel zone plate, which
7 is used as an objective lens for an image magnification of 44x by the first order diffraction
8 mode. Conjugated with a 20x downstream optical magnification, the TXM provides a total
9 magnification of 880x with a field of view of $15 \times 15 \mu m^2$. By acquiring a series of 2D
10 images with the sample rotated 1° stepwise, 3-D tomography datasets is later
11 reconstructed based on 151 sequential image frames that are captured with azimuth
12 angle rotating from -75° to $+75^\circ$.

13

14 **Image acquisition for 3-D tomography**

15 Under the most frequently used absorption contrast mode, 2-D images are
16 recorded based on the projection of the different X-ray absorption coefficient integration
17 along the optical pathway through samples on a detector. The absorption mode is useful
18 for materials of high absorption coefficient, such as minerals or high atomic number
19 materials, but it is poor for the observation of low atomic number materials, such as
20 organic or polymer materials. In order to recognize the OC structure more accurately, 2-

1 D/3-D images for the same sample region are recorded using absorption contrast and
2 phase contrast modes, respectively.

3 In the phase contrast mode, the gold-made phase ring positioned at the back-focal
4 plane of the zone plate is used to retard or advance the phase of the non-diffractive light
5 by $\pi/2$, generating (Zernike's) phase contrast images recording at the detector. The light
6 diffracted by specimen is interfered with the retarded non-diffractive light, generating
7 phase contrast image. The intensity difference in a phase contrast image shows the
8 combination of optical phase difference and absorption difference through specimens.
9 This ability is especially important for the observation of OC which has a low X-ray
10 absorption coefficient.

11

12 **3-D reconstruction and analysis**

13 Three dimensional tomography reconstruction is performed using homemade
14 software, which is coded based on iterative image registration (Faproma) (Wang et al.
15 2017) and filtered back projection (FBP) reconstruction algorithms. Firstly, a serial of
16 single TXM image captured from -75° to $+75^\circ$ at rotational increments of 1° is loaded to
17 do image registration automatically using Faproma algorithm. Finally, the reconstruction
18 is processed using FBP algorithm. The reconstructed dataset is exported in cross-
19 sections, and later used for 3-D visualization using *Amira*. The intensity contrast of
20 reconstructed datasets is inversed for better visualization. Compositions with higher
21 absorption coefficients are shown in higher intensity and [those](#) with low absorption

1 coefficients are shown in lower intensity. The exported cross-section of 3-D tomography
2 (reconstructed datasets) shows the real distribution details and boundary interplay of OC
3 and mineral particles. The final 3-D tomographic structures for visualization and
4 illustration are generated using *Amira* 3-D software for image post-process and
5 computation (Fig. S1).

6

7 **Elemental mapping by SEM-EDS**

8 For correlated spatial distribution of selected elements (C, O, Fe, Al [etc](#)) in natural
9 OC particles from [the](#) high mountain soil, a low-vacuum scanning electron microscope
10 (JEOL W-LVSEM, JSM-6360LV) equipped with an energy dispersive X-ray spectrometer
11 (Oxford EDS) and a cathodoluminescence (CL) image detector (Gatan mini-CL) was used
12 for elemental mapping, at an accelerating voltage of 15 KeV.

13

14 **X-ray Diffraction for Mineralogy**

15 To analyze the forms of minerals associated with natural OC, particulate OC (with
16 minerals on [the](#) surface and embedded inside) was grounded and injected into capillary
17 tubes (Special Glass 10, Hampton Research, CA) for synchrotron high resolution X-ray
18 diffraction analysis at 09A beamline at Taiwan Photon Source (TPS), which is equipped
19 with a set of high-resolution monochromator (HRM). The wavelength is 0.8266 Å at the
20 energy of 15 KeV. The XRD spectra were recorded under room temperature for 240s
21 accumulation time and specific X-ray diffraction peaks and patterns were assigned ICDD
22 using PDF-2/4 program.

1

2 **Carbon functionality and interfacial mineral forms using SR-FTIR**

3 For FTIR analysis, mineral-bearing OC (NH) particles were grounded, dried (60 °C
4 overnight), and mixed with potassium bromide (KBr) at a ratio of 1:100, and molded into
5 disks using a hydraulic press. During the pressing process, a vacuum pump was used for
6 evacuating air and water. The samples were measured using Infrared
7 Microspectroscopy (IMS) at the BL14A1 beamline of the National Synchrotron Radiation
8 Research Center (NSRRC), Taiwan. The FTIR spectra were collected up to 1024 scans
9 in the mid-infrared range of 4000-400 cm^{-1} with a spectral resolution of 4 cm^{-1} , using a
10 FTIR spectrometer (Nicolet 6700, Thermo Fisher Scientific, Madison, WI, USA) with a
11 self-equipped light source. The automatic atmospheric suppression function in OMNIC
12 (OMNIC 9.2, 2012; Thermo Fisher Scientific Inc., Waltham, MA, USA) for bulk sample
13 analysis was activated for data analysis, to eliminate the rovibration absorptions of CO_2
14 and water vapor in ambient air.

15

16 **Results and Discussions**

17 **Distinguish the fine structure of BC and boundary interplay with mineral nano** 18 **particles**

19 High resolution 2-D X-ray photographs were captured for the identical regions in
20 lab-made BC and nano mineral consortium using dual-scan absorption contrast and
21 phase contrast modes (Fig. 1, a, e). The cross-section views exported from the

1 reconstructed 3-D datasets reveal subtle details of BC and mineral nano particles, and
2 clearly outline the fine boundary of BC and the distribution of TiO₂ nano particles (Fig. 1).
3 The shape, size, and distribution of mineral nano particles can be identified accurately
4 using absorption contrast mode due to their high X-ray absorptivity (Fig.1, b, c and d). In
5 comparison, the BC structure and contour of its boundary can be revealed much more
6 clearly using phase contrast mode (Fig.1, f, g and h). However, the bright halo artifacts in
7 phase-contrast image enhance the intensity of margin texture for nano minerals, and may
8 lead to overestimation of their volume (Fig. 1, e, f, g and h). Use of dual-scan mode allows
9 cross-checking of details and validation.

10 Cross-section views of the reconstructed 3-D tomography share consistent and
11 comparable features of BC and nano minerals in multi-angles (Fig. 2). According to the
12 display of different slicing planes (XY, XZ, YZ), it can be recognized that TiO₂ nano
13 particles deposit inside BC only sporadically contact with BC boundary (Fig. 2, b, e, c,
14 and f) due to the treatment of dry deposition. The nano scale gap between BC and nano
15 minerals has been clearly observed in absorption and phase-contrast images (Fig. 2, b,
16 e, c, and f). It is feasible to calculate the interplay surface and mineral volume
17 quantitatively by examining each cross-section views in a selected region. Our approach
18 is a success in thorough exploration of OC and minerals 3-D distribution, and verification
19 of their real in-situ spatial correlation under nano scale resolution.

20

21 **3-D tomography for illustrating in-situ distribution of BC and mineral nano particles**

1 3-D tomography for visualization has been computed and generated to illustrate
2 the spatial correlation between BC and minerals based on post-process of reconstructed
3 3-D datasets. Unprecedented details of 3-D in-situ distribution of BC and mineral nano
4 particles are revealed in computed 3-D tomography (Fig. 3; Fig. SMOV1, 2). Results from
5 absorption mode and phase contrast mode are consistent and comparable. The fine
6 boundary feature of BC is contoured to a more completeness in the phase contrast mode.
7 The OC was rendered by transparent mode and high absorptivity materials (such as
8 minerals and gold particles) were rendered by solid mode with various colors. All
9 renderings are combined to visualize their interaction. The illustration of 3-D computed
10 tomography allows randomly tilted and set angles for image and animated video exports,
11 thus any region of interest inside a specimen may be explored thoroughly.

12 The lab-made consortium was successfully tested by this dual-scan methodology
13 using both absorption contrast and phase-contrast acquisition modes (Figs. 1, 2, 3). Low
14 temperature BC, which is more similar to natural OC (especially recalcitrant OC) than that
15 made at high temperature, was especially made to test its applicability under absorption
16 contrast mode. Results show that the fine structure and boundary of low temperature BC
17 can be clearly observed under absorption contrast mode. Thus for environmental OC
18 samples, the use of absorption contrast mode is probably sufficient for capturing organo-
19 mineral features.

20 Different from field samples, the minerals observed within the lab-made consortium
21 often distribute in clusters and are only sparsely in association with BC surface. The
22 preservation of plant-like structures in BC could play a role for carbon stabilization in

1 natural environment, as their porosity and reactive surface provide large areas and sites
2 for mineral coating, which may contribute to their long residence and physical endurance
3 (Eusterhues et al., 2008; Rasmussen et al., 2005; Rawal et al., 2016).

4

5 **Interplay of OC and minerals and C stabilization in high mountain soil**

6 Nano scale 3-D tomography revealed a high heterogeneity within natural OC-
7 mineral consortium, and most of the particulate OC surface is coated by minerals.
8 ~~provides new insight for the mineral physical protection mechanism of OC in soil.~~ Natural
9 OC exhibited strong organo-mineral association on its surface at nano scale ~~in high~~
10 ~~mountain soil~~ (Fig. 4; Fig. SMOV3). Abundant ~~short-range order~~ SRO minerals in forms of
11 subhedral particle or anhedral nano-aggregates /clusters have direct association ~~contact~~
12 with the boundary of OC₁ and develop coating on the tracheid surface (Fig. 4 b and c)
13 (Mikutta et al., 2006). Sheet-like mineral coating is observed on OC surface, which are
14 dense and thin layers, likely originated from absorption (Fig. 4 b, Fig. S2). ~~Another distinct~~
15 ~~texture is recognized as nano-aggregates/clusters of various shapes, possibly formed by~~
16 ~~OC-mineral co-precipitation. Mineral aggregation by poorly crystalline nano particles~~
17 ~~renders natural sub-micron porosity, which may contribute to elevated sorption capacity~~
18 ~~in soil (Rawal et al., 2016).~~ The densely-packed mineral texture suggested significant
19 physical protection on OC surface (Kaiser and Guggenberger, 2007). The sorbed
20 minerals not only ~~can~~ form physical protection, but ~~also~~ could also shield OC from
21 chemical weathering (Mikutta et al., 2006). The key working minerals for OC-mineral
22 interplay are essentially SRO mineral nano particles, and/or poorly crystalline submicron

1 [size clay minerals, instead of crystalline, micron/clay-size minerals.](#) Another distinct
2 [texture is recognized as nano-aggregates/clusters of various shapes, indicating possible](#)
3 [OC-mineral co-precipitation \(Fig. 4 b, Fig. S3\). Mineral aggregation by poorly crystalline](#)
4 [nano particles renders natural sub-micron porosity, which may contribute to elevated](#)
5 [sorption capacity in soil \(Rawal et al., 2016\).](#)

6 The nature of associated minerals was confirmed to be mainly [SRO](#) Fe
7 oxyhydroxides, specifically ferrihydrite (ICDD 01-073-8408), goethite (ICDD 01-073-
8 6522), lepidocrocite (ICDD 00-044-1415), and quartz (ICDD 00-033-1161) (Fig. 5; Table
9 S1), analyzed using high resolution synchrotron-based [X-ray diffraction](#). Quartz may
10 be at most a minor component on OC surface, considering their chemistry and particle
11 size. Yet siliceous mineral surfaces may [become](#) coated with a veneer of hydrous Al- and
12 Fe- oxides, which could confer net positive charge and promote their reactivity in tropical
13 environments (Chen et al., 2014a; Sposito, 1989).

14 Considering their high surface area and reactivity, the abundant nano [size](#) Fe
15 oxyhydroxides could play a significant role for OC long-term stabilization through
16 chemical bonding and physical shielding (Eusterhues et al., 2005; Kaiser et al., 2002;
17 Kiem and Kogel-Knabner, 2002; Mikutta et al., 2006), [as well as cation sorption in soil,](#)
18 and contribute to [the](#) longevity of OC in high mountain soil. According to elemental
19 mapping [results](#), aluminosilicates may also be present, however, their portion and
20 [crystallization](#) level should be low due to their minimal signal in the XRD spectra (Figs. 5,
21 6). The FTIR analyses reveal the chemistry of organo-mineral association (Fig. 7; Table
22 S2). The aged OC is highly aromatic when at the same time highly reactive, [likely](#)

1 [originated from pyrogenic C](#), as broad bands [are observed](#) centered at 1596 cm⁻¹ and
2 1706 cm⁻¹ for aromatic C=C stretching and [carboxylic](#) ν C=O, (Özçimen and Ersoy-
3 Meriçboyu, 2010; Sharma et al., 2004). Both aromatic and carboxyl C functional groups
4 normally have high affinity with Fe (III) (Mikutta et al., 2007; Zhao et al., 2016). [Broad](#)
5 [bands indicate](#) a significant degree of association between OC and minerals (Chen et al.,
6 2016; Gu et al., 1994; Kaiser and Guggenberger, 2007). The sorption of OC to Fe
7 oxyhydroxides through organo-mineral multiple complex bonds [such as 'ligand exchange'](#)
8 [could occupy their](#) reactive surface sites ~~on OC and Fe oxyhydroxides~~, ~~tune down their~~
9 ~~activity~~ and enhance their respective stabilization (Chorover and Amistadi, 2001; Cornell
10 and Schwertmann, 2006; Hall et al., 2016; Kaiser and Guggenberger, 2007; Mikutta et
11 al., 2007). The discovery of [short-range-order SRO](#) mineral ferrihydrite in air-dried OC
12 particles and later ground-samples indirectly validates its stabilization due to organo-
13 mineral interplay. As a [SRO](#)/metastable mineral, ferrihydrite is hard to estimate accurately
14 in dry soil samples due to its transient nature and the limitation of traditional extraction
15 and spectroscopic methods (Cornell and Schwertmann, 2006). The specific mineral
16 [phase](#) in direct contact with OC on surface at nano scale warrants future study (Fig.
17 SMOV3). In-situ mineral mapping of different [SRO minerals](#)/-Fe oxyhydroxide on OC
18 surface will provide mechanistic [understanding](#) on OC stabilization. Mineral physical
19 protection on OC may represent the end stage of carbon stabilization, especially in a
20 weak leaching and weathering environment.

21 Our in-situ description of organo-mineral interplay at nano scale provides direct
22 evidence on the [importance](#) of mineral physical protection for OC long term stabilization.

1 High amounts of ferrihydrite and other Fe oxyhydroxides were also found associated with
2 lignin-like OC in soil under an aquic moisture regime (Eusterhues et al., 2011). The
3 abundance of mineral nano particles, and their high heterogeneity and short-range-order
4 nature could be common in humid environment, however, they could have been seriously
5 underestimated by traditional analysis methods, such as electron microscopy, X-ray
6 diffraction and fractionation approaches, which focus on clay-size minerals (Mikutta et al.,
7 2005). Mineral physical protection for OC stabilization may be more important than
8 previous understanding. More research is proposed to explore: i) whether it is a general
9 phenomenon that the minerals interact with OC are essentially SRO mineral nano particle
10 and or poorly crystalline submicron size clay minerals, ii) whether the major mineral for C
11 stabilization is nano size SRO minerals instead of clay-size minerals in soils. Perspective
12 on C stabilization and saturation should be revolutionized to take the role of SRO minerals
13 into account in modelling soil C dynamics, in addition to parameters such as clay type
14 and content.

15 In summary, a high resolution 3-D tomography tool is required for exploring the in-
16 situ interplay of OC and mineral nano particles in natural environment. Nano scale 3-D
17 tomography provides direct evidence and new insight for the mineral physical protection
18 mechanism of OC in soil. This high resolution 3-D tomography approach is a promising
19 technique for probing the multi interfacial features between OC and minerals in lab and
20 field samples, and may provide new perspective on the fate of nano particles including
21 heavy metals in natural environments.

22

1

2 **Figure Captions**

3 **Figure 1.** [The 2-D X-ray images for BC and mineral nano particle consortium. Two images](#)
4 [are taken for the same region using absorption contrast mode \(a\) and phase contrast](#)
5 [mode \(e\), respectively.](#) Cross-section views of the reconstructed 3-D tomography under
6 each mode at different depths relative to the position of gold nano particle along Z-axis
7 as a reference. **(b)** and **(f)** are sections extracted at the position of the gold particle. **(c)**
8 and **(g)** are sections extracted at 800 nm above the gold particle. **(d)** and **(h)** are sections
9 extracted at 800 nm below the gold particle. The scale bar is 5 μm .

10 **Figure 2.** Three-directional orthogonal sections of lab-made BC and mineral nano particle
11 consortium. The upper row sections are extracted from absorption contrast tomography
12 **(a, b, c)**, and the lower row sections are extracted from phase contrast tomography **(d, e,**
13 **f)**, specifically **(a)** and **(d)** are for XY plane, **(b)** and **(e)** are for YZ plane, and **(c)** and **(f)**
14 are for XZ plane. The scale bar is 5 μm .

15 **Figure 3.** 3-D tomography illustration of lab-made BC and mineral nano particle
16 consortium observed at -45° **(a, d)**, 0° **(b, e)**, and $+45^\circ$ **(c, f)** azimuthal viewing angles
17 under absorption contrast **(a, b, c)** and phase contrast mode **(d, e, f)**. The scale bar is 5
18 μm .

19 **Figure 4.** Three-directional orthogonal sections of high mountain mineral-bearing OC
20 from absorption contrast tomography **(a** for XY plane, **b** for XZ plane, and **c** for YZ plane). .
21 The scale bar is 5 μm . Minerals mainly present two types of textures, subhedral particles

1 and anhedral nano-aggregates. The lower row images highlight the free surface of
2 specimen (red line in **d**), the boundary of OC (green dotted-line in **e**), and the subhedral
3 mineral particles (pink arrow in **e** and **f**)

4 **Figure 5.** The X-ray diffraction pattern of minerals within OC particles from high mountain
5 soil. Highly reactive Fe oxyhydroxides are identified and denoted with lines of different
6 colors: ferrihydrite (ICDD 01-073-8408, orange), goethite (ICDD 01-073-6522, blue), and
7 lepidocrocite (ICDD 00-044-1415, green). Q stands for Quartz (ICDD 00-033-1161).
8 Details are included in Table S1.

9 **Figure 6.** Elementary mapping by SEM-EDS for mineral-bearing OC from high mountain
10 soil. Left: SEM backscattering image (The bright spots inside are gold nano particles for
11 coating). Right: Elemental mapping of C, O, Fe and Al. Scale bars are 20 μm .

12 **Figure 7.** The FTIR spectra for the chemistry of organo-mineral association. The aged
13 OC is highly aromatic (1596 and 1386 cm^{-1}), and highly reactive with obvious carboxyl
14 functional group (1706 cm^{-1}). The broad bands point to possible significant degree of
15 association between OC and minerals. Some minor bands near 1274 , 1062 , 1024 , and
16 989 cm^{-1} indicate the lignin-derived nature of OC. Those bands near 476 , 534 , 798 , 910
17 and 1025 cm^{-1} have similar characteristics of soil inorganic/mineral matrix. More details
18 are included in Table S2.

19

20

21 **Acknowledgement**

1 We thank Dr. Chung-Ho Wang for kind support, the technical support from Ms. Hsueh-
2 Chi Wang (TXM, TLS-BL01B01); Dr. Yao-Chang Lee and Ms. Pei-Yu Huang (FTIR, TLS-
3 BL14A1); and Dr. Hwo-Shuenn Sheu and Dr. Yu-Chun Chuang (XRD, TPS-09A1) at the
4 end-stations of NSRRC (Taiwan), the help for SEM-EDS analysis from Dr. Yoshiyuki
5 Iizuka (Academia Sinica), the SC specimen from Dr. Chih-Hsin Cheng (National Taiwan
6 University), the TiO₂ nano particles from Dr. Yen-Hua Chen (NCKU, the department of
7 Earth Sciences), and Dr. Chia-Chuan Liu, the former and current members of the NCKU
8 Global Change Geobiology Carbon Laboratory for help and support.

9

10

11 **Funding Sources**

12 BQ Liang and CC Wang acknowledged the funding support from Taiwan Ministry of
13 Science and Technology (MOST 102-2116-M-006-018-MY2, MOST 105-2116-M-006-
14 010-, and MOST 105-2112-M-213-001).

15

16

17 **References**

18 Alexandre, A., Basile-Doelsch, I., Delhaye, T., Borshneck, D., Mazur, J. C., Reyerson,
19 P., and Santos, G. M.: New highlights of phytolith structure and occluded carbon
20 location: 3-D X-ray microscopy and NanoSIMS results, *Biogeosciences*, 12, 863-
21 873, 2015.

22 Baldock, J. A. and Skjemstad, J. O.: Role of the soil matrix and minerals in protecting
23 natural organic materials against biological attack, *Org. Geochem.*, 31, 697-710,
24 2000.

- 1 Bond, T. C., Doherty, S. J., Fahey, D. W., Forster, P. M., Bernsten, T., DeAngelo, B. J.,
2 Flanner, M. G., Ghan, S., Karcher, B., Koch, D., Kinne, S., Kondo, Y., Quinn, P. K.,
3 Sarofim, M. C., Schultz, M. G., Schulz, M., Venkataraman, C., Zhang, H., Zhang,
4 S., Bellouin, N., Guttikunda, S. K., Hopke, P. K., Jacobson, M. Z., Kaiser, J. W.,
5 Klimont, Z., Lohmann, U., Schwarz, J. P., Shindell, D., Storelvmo, T., Warren, S.
6 G., and Zender, C. S.: Bounding the role of black carbon in the climate system: A
7 scientific assessment, *J. Geophys. Res-Atmos.*, 118, 5380-5552, 2013.
- 8 Bousige, C., Ghimbeu, C. M., Vix-Guterl, C., Pomerantz, A. E., Suleimenova, A.,
9 Vaughan, G., Garbarino, G., Feygenson, M., Wildgruber, C., Ulm, F.-J., Pellenq, R.
10 J. M., and Coasne, B.: Realistic molecular model of kerogen's nanostructure,
11 *Nature Materials*, 15, 576, 2016.
- 12 Chen, C., Dynes, J. J., Wang, J., Karunakaran, C., and Sparks, D. L.: Soft X-ray
13 Spectromicroscopy Study of Mineral-Organic Matter Associations in Pasture Soil
14 Clay Fractions, *Environ. Sci. Technol.*, 48, 6678-6686, 2014a.
- 15 Chen, C. P., Cheng, C. H., Huang, Y. H., Chen, C. T., Lai, C. M., Menyailo, O. V., Fan,
16 L. J., and Yang, Y. W.: Converting leguminous green manure into biochar: changes
17 in chemical composition and C and N mineralization, *Geoderma*, 232, 581-588,
18 2014b.
- 19 Chen, K.-Y., Chen, T.-Y., Chan, Y.-T., Cheng, C.-Y., Tzou, Y.-M., Liu, Y.-T., and Teah,
20 H.-Y.: Stabilization of Natural Organic Matter by Short-Range-Order Iron
21 Hydroxides, *Environ. Sci. Technol.*, 50, 12612-12620, 2016.
- 22 Chorover, J. and Amistadi, M. K.: Reaction of forest floor organic matter at goethite,
23 birnessite and smectite surfaces, *Geochim. Cosmochim. Acta*, 65, 95-109, 2001.
- 24 Cornell, R. M. and Schwertmann, U.: *The Iron Oxides: Structure, Properties, Reactions,*
25 *Occurrences and Uses*, Wiley, 2006.
- 26 Cusack, D. F., Chadwick, O. A., Hockaday, W. C., and Vitousek, P. M.: Mineralogical
27 controls on soil black carbon preservation, *Global Biogeochem. Cy.*, 26, 2019,
28 2012.
- 29 Eusterhues, K., Rennert, T., Knicker, H., Kögel-Knabner, I., Totsche, K. U., and
30 Schwertmann, U.: Fractionation of Organic Matter Due to Reaction with

1 Ferrihydrite: Coprecipitation versus Adsorption, *Environ. Sci. Technol.*, 45, 527-
2 533, 2011.

3 Eusterhues, K., Rumpel, C., and Kögel-Knabner, I.: Organo-mineral associations in
4 sandy acid forest soils: importance of specific surface area, iron oxides and
5 micropores, *Eur. J. Soil Sci.*, 56, 753-763, 2005.

6 Eusterhues, K., Wagner, F. E., Häusler, W., Hanzlik, M., Knicker, H., Totsche, K. U.,
7 Kögel-Knabner, I., and Schwertmann, U.: Characterization of Ferrihydrite-Soil
8 Organic Matter Coprecipitates by X-ray Diffraction and Mössbauer Spectroscopy,
9 *Environ. Sci. Technol.*, 42, 7891-7897, 2008.

10 Gu, B. H., Schmitt, J., Chen, Z. H., Liang, L. Y., and Mccarthy, J. F.: Adsorption and
11 Desorption of Natural Organic-Matter on Iron-Oxide - Mechanisms and Models,
12 *Environ. Sci. Technol.*, 28, 38-46, 1994.

13 Hall, S. J., Silver, W. L., Timokhin, V. I., and Hammel, K. E.: Iron addition to soil
14 specifically stabilized lignin, *Soil Biol. Biochem.*, 98, 95-98, 2016.

15 Jeffery, S., Bezemer, T. M., Cornelissen, G., Kuyper, T. W., Lehmann, J., Mommer, L.,
16 Sohi, S. P., van de Voorde, T. F. J., Wardle, D. A., and van Groenigen, J. W.: The
17 way forward in biochar research: targeting trade-offs between the potential wins,
18 *GCB. Bioenergy*, 7, 1-13, 2015.

19 Kaiser, K., Eusterhues, K., Rumpel, C., Guggenberger, G., and Kogel-Knabner, I.:
20 Stabilization of organic matter by soil minerals - investigations of density and
21 particle-size fractions from two acid forest soils, *J. Plant Nutr. Soil Sci.*, 165, 451-
22 459, 2002.

23 Kaiser, K. and Guggenberger, G.: Sorptive stabilization of organic matter by
24 microporous goethite: sorption into small pores vs. surface complexation, *Eur. J.*
25 *Soil Sci.*, 58, 45-59, 2007.

26 Kiem, R. and Kogel-Knabner, I.: Refractory organic carbon in particle-size fractions of
27 arable soils II: organic carbon in relation to mineral surface area and iron oxides in
28 fractions < 6 μ m, *Org. Geochem.*, 33, 1699-1713, 2002.

1 Kinyangi, J., Solomon, D., Liang, B., Lerotic, M., Wirick, S., and Lehmann, J.:
2 Nanoscale Biogeochemical Complexity of the Organomineral Assemblage in Soil, *Soil Sci.*
3 *Soc. Am. J.*, 70, 1708-1718, 2006.

4 Kleber, M., Sollins, P., and Sutton, R.: A conceptual model of organo-mineral
5 interactions in soils: self-assembly of organic molecular fragments into zonal
6 structures on mineral surfaces, *Biogeochemistry*, 85, 9-24, 2007.

7 Kuhlbusch, T. A. J.: Black carbon and the carbon cycle, *Science*, 280, 1903-1904, 1998.

8 Kuo, C.-H., Chu, Y.-T., Song, Y.-F., and Huang, M. H.: Cu₂O Nanocrystal-Templated
9 Growth of Cu₂S Nanocages with Encapsulated Au Nanoparticles and In-Situ
10 Transmission X-ray Microscopy Study, *Adv. Funct. Mater.*, 21, 792-797, 2011.

11 Lehmann, J., Kinyangi, J., and Solomon, D.: Organic matter stabilization in soil
12 microaggregates: implications from spatial heterogeneity of organic carbon
13 contents and carbon forms, *Biogeochemistry*, 85, 45-57, 2007.

14 Lehmann, J., Solomon, D., Kinyangi, J., Dathe, L., Wirick, S., and Jacobsen, C.: Spatial
15 complexity of soil organic matter forms at nanometre scales, *Nat. Geosci.*, 1, 238-
16 242, 2008.

17 Liang, B., Lehmann, J., Solomon, D., Kinyangi, J., Grossman, J., O'Neill, B., Skjemstad,
18 J. O., Thies, J., Luizao, F. J., Petersen, J., and Neves, E. G.: Black Carbon
19 increases cation exchange capacity in soils, *Soil Sci. Soc. Am. J.*, 70, 1719-1730,
20 2006.

21 Liang, B., Lehmann, J., Solomon, D., Sohi, S., Thies, J. E., Skjemstad, J. O., Luizão, F.
22 J., Engelhard, M. H., Neves, E. G., and Wirick, S.: Stability of biomass-derived
23 black carbon in soils, *Geochim. Cosmochim. Acta*, 72, 6069-6078, 2008.

24 Mikutta, R., Kleber, M., and Jahn, R.: Poorly crystalline minerals protect organic carbon
25 in clay subfractions from acid subsoil horizons, *Geoderma*, 128, 106-115, 2005.

26 Mikutta, R., Kleber, M., Torn, M. S., and Jahn, R.: Stabilization of Soil Organic Matter:
27 Association with Minerals or Chemical Recalcitrance?, *Biogeochemistry*, 77, 25-56,
28 2006.

- 1 Mikutta, R., Mikutta, C., Kalbitz, K., Scheel, T., Kaiser, K., and Jahn, R.: Biodegradation
2 of forest floor organic matter bound to minerals via different binding mechanisms,
3 *Geochim. Cosmochim. Acta*, 71, 2569-2590, 2007.
- 4 Özçimen, D. and Ersoy-Meriçboyu, A.: Characterization of biochar and bio-oil samples
5 obtained from carbonization of various biomass materials, *Renew. Energy*, 35,
6 1319-1324, 2010.
- 7 Rasmussen, C., Torn, M. S., and Southard, R. J.: Mineral assemblage and aggregates
8 control carbon dynamics in a California conifer forest, *Soil Sci. Soc. Am. J.*, 69,
9 1711-1721, 2005.
- 10 Rawal, A., Joseph, S. D., Hook, J. M., Chia, C. H., Munroe, P. R., Donne, S., Lin, Y.,
11 Phelan, D., Mitchell, D. R. G., Pace, B., Horvat, J., and Webber, J. B. W.: Mineral-
12 Biochar Composites: Molecular Structure and Porosity, *Environ. Sci. Technol.*, 50,
13 7706-7714, 2016.
- 14 Schmidt, M. W. I.: Biogeochemistry: Carbon budget in the black, *Nature*, 427, 305-307,
15 2004.
- 16 Sharma, R. K., Wooten, J. B., Baliga, V. L., Lin, X., Geoffrey Chan, W., and Hajaligol,
17 M. R.: Characterization of chars from pyrolysis of lignin, *Fuel*, 83, 1469-1482, 2004.
- 18 Sollins, P., Kramer, M. G., Swanston, C., Lajtha, K., Filley, T., Aufdenkampe, A. K.,
19 Wagai, R., and Bowden, R. D.: Sequential density fractionation across soils of
20 contrasting mineralogy: evidence for both microbial- and mineral-controlled soil
21 organic matter stabilization, *Biogeochemistry*, 96, 209-231, 2009.
- 22 Solomon, D., Lehmann, J., Harden, J., Wang, J., Kinyangi, J., Heymann, K.,
23 Karunakaran, C., Lu, Y., Wirick, S., and Jacobsen, C.: Micro- and nano-
24 environments of carbon sequestration: Multi-element STXM-NEXAFS
25 spectromicroscopy assessment of microbial carbon and mineral associations,
26 *Chem. Geol.*, 329, 53-73, 2012.
- 27 Sposito, G.: *The Chemistry of Soils*, Oxford University Press, 1989.
- 28 Torn, M. S., Trumbore, S. E., Chadwick, O. A., Vitousek, P. M., and Hendricks, D. M.:
29 Mineral control of soil organic carbon storage and turnover, *Nature*, 389, 170-173,
30 1997.

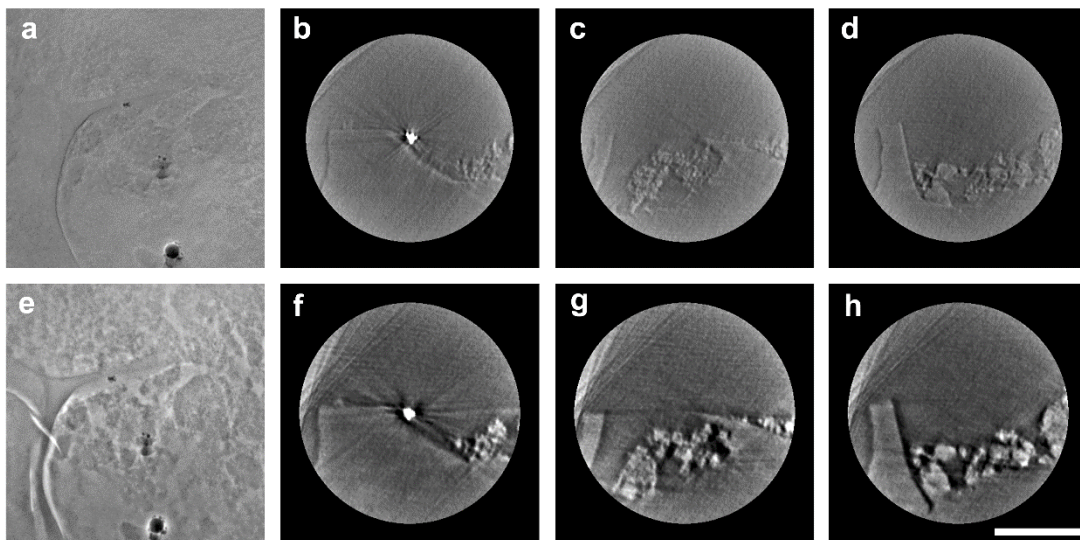
1 Vogel, C., Mueller, C. W., Hoschen, C., Buegger, F., Heister, K., Schulz, S., Schloter,
2 M., and Kogel-Knabner, I.: Submicron structures provide preferential spots for
3 carbon and nitrogen sequestration in soils, *Nat. Commun.*, 5, 2947, 2014.

4 Wang, C.-C., Song, Y.-F., Song, S.-R., Ji, Q., Chiang, C.-C., Meng, Q., Li, H., Hsiao, K.,
5 Lu, Y.-C., Shew, B.-Y., Huang, T., and Reisz, R. R.: Evolution and Function of
6 Dinosaur Teeth at Ultramicrostructural Level Revealed Using Synchrotron
7 Transmission X-ray Microscopy, *Sci. Rep.*, 5, 15202, 2015.

8 Zbik, M. S., Frost, R. L., Song, Y. F., Chen, Y. M., and Chen, J. H.: Transmission X-ray
9 microscopy reveals the clay aggregate discrete structure in aqueous environment,
10 *J. Colloid Interf. Sci.*, 319, 457-461, 2008.

11 Zhao, Q., Poulson, S. R., Obrist, D., Sumaila, S., Dynes, J. J., McBeth, J. M., and Yang,
12 Y.: Iron-bound organic carbon in forest soils: quantification and characterization,
13 *Biogeosciences*, 13, 4777-4788, 2016.

14
15
16
17
18
19

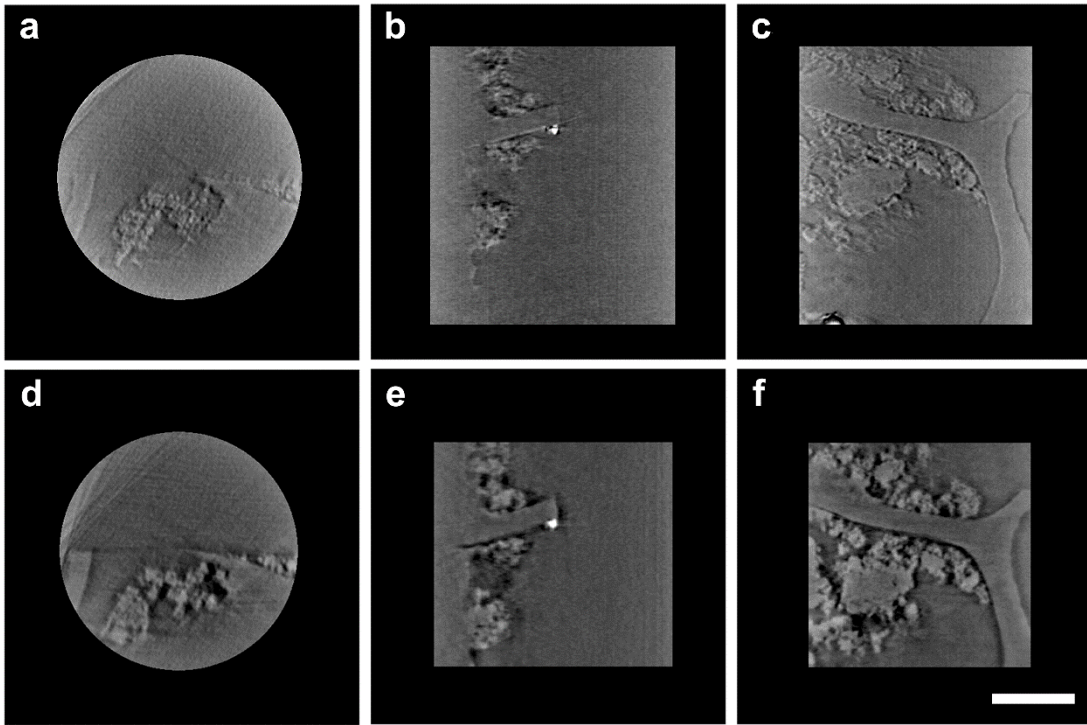


20

1 **Figure 1.**

2

3

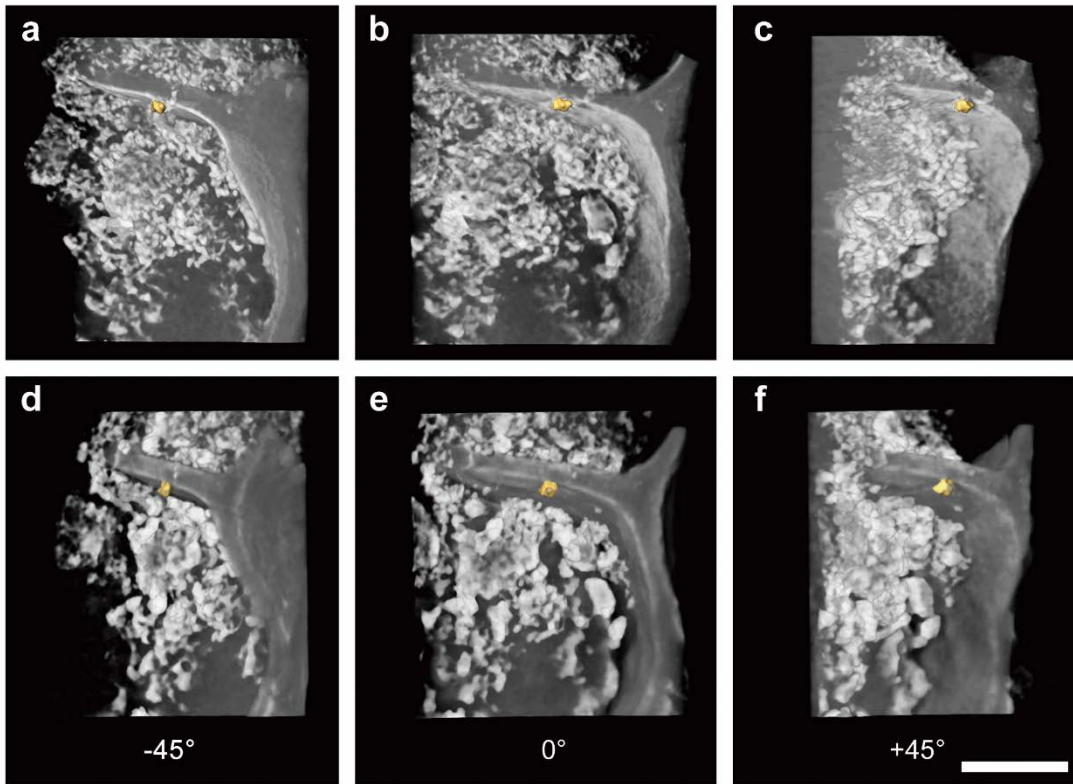


4

5 **Figure 2.**

6

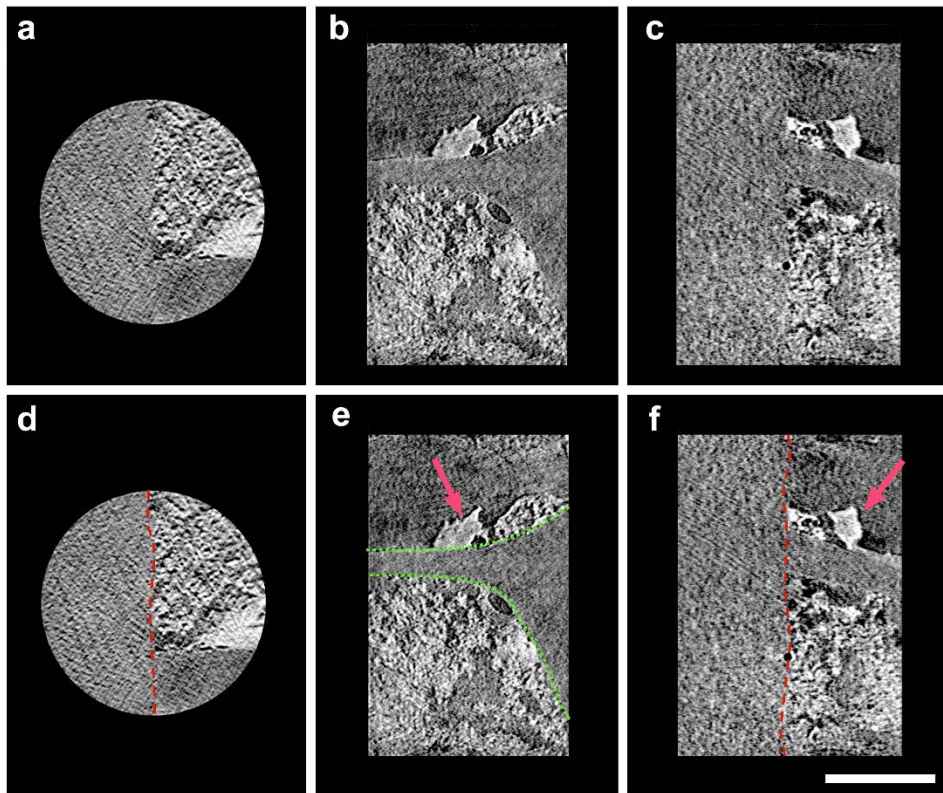
7



1

2 **Figure 3.**

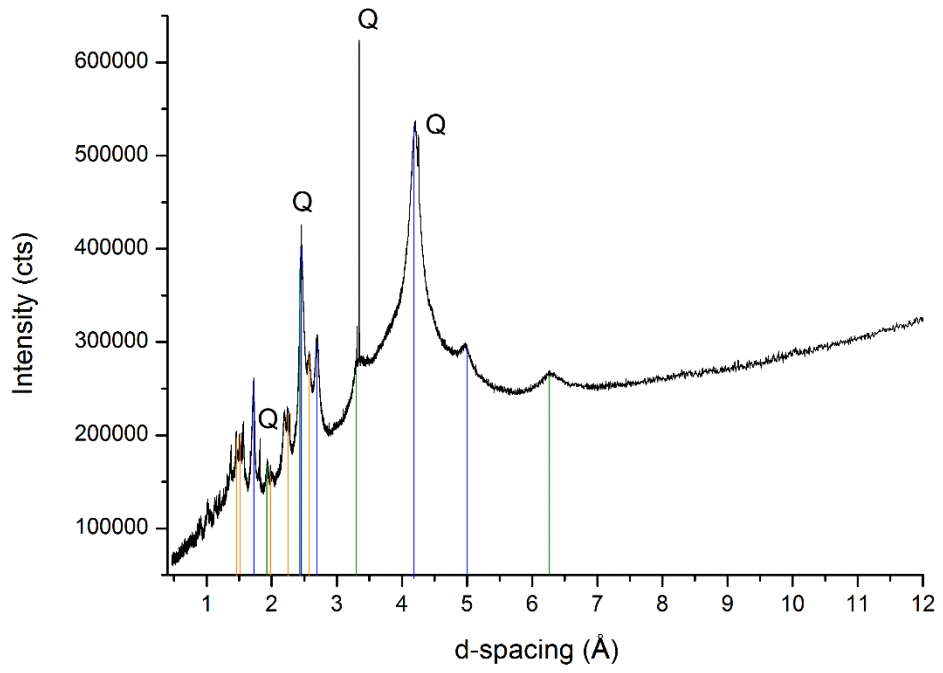
3



1

2

3 **Figure 4.**

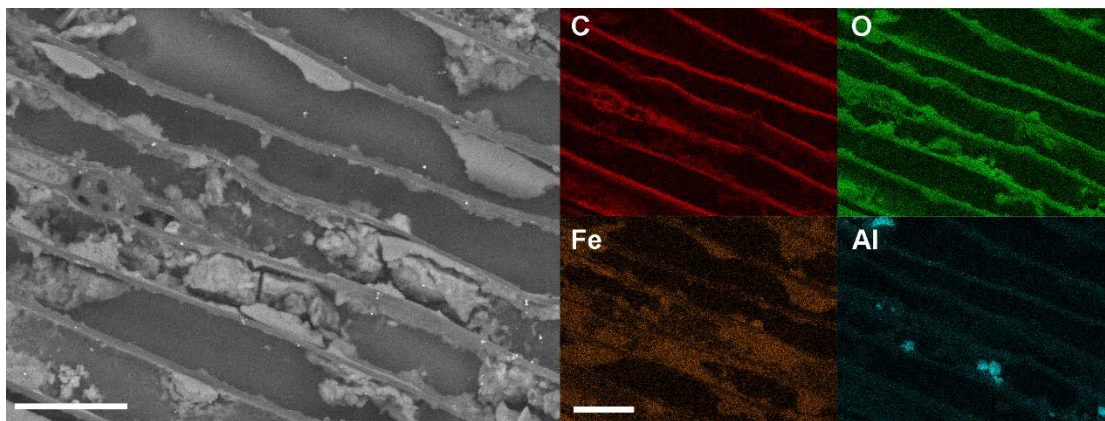


1

2 **Figure 5.**

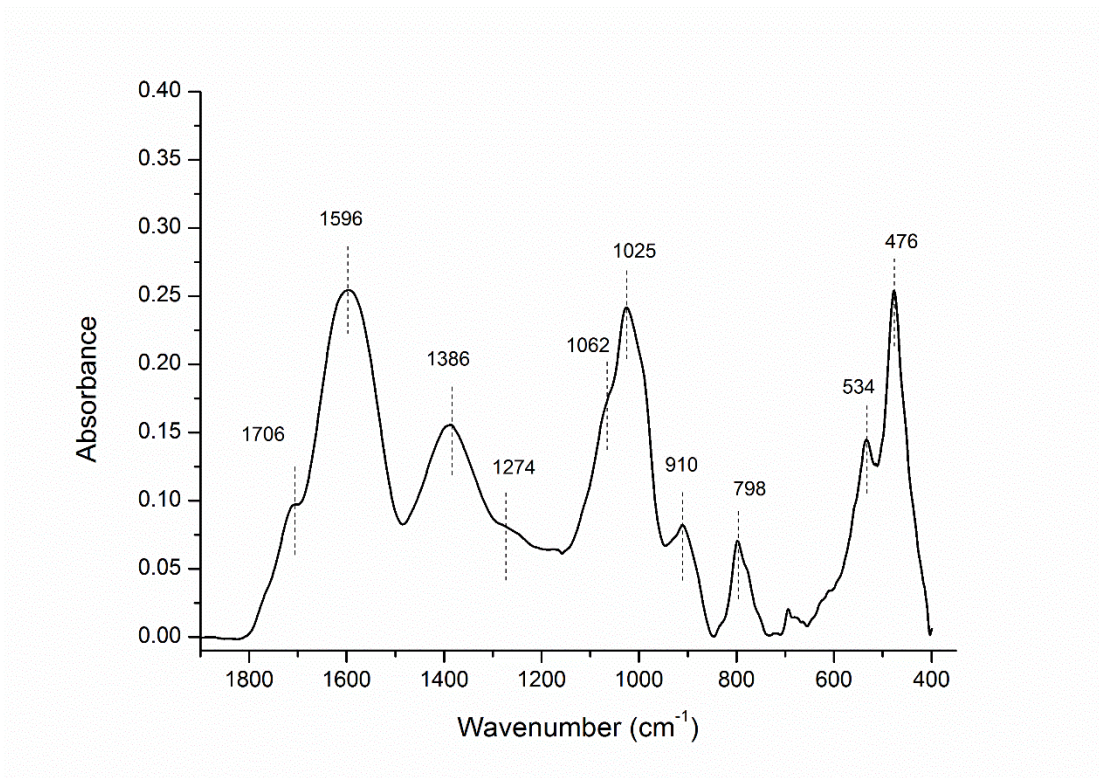
3

4



5

6 **Figure 6.**



1

2 **Figure 7.**

3